

The Seasonal Behavior of the Refractive Index of the Ionosphere over the Equatorial Region

A. YESİL¹, S. KARATAY², S. SAGIR³, K. KURT⁴

¹Firat University, Science Faculty, Department of Physics, Elazig, Turkey

²Kastamonu University, Department of Physics, Kastamonu, Turkey

³Muş Alparslan University, Department of Physics, Mus, Turkey

⁴Dicle University, Science Faculty, Department of Physics, Diyarbakir, Turkey

ayesil@firat.edu.tr

(Received: 08.10.2012; Accepted: 03.03.2013)

Abstract

In this study, the seasonal behavior of the refractive index of the ionosphere over equator region is investigated both for collisional and collisionless cases by using the real geometry of Earth's magnetic field for north hemisphere with respect to latitudes. It is observed that there is a harmony between the behavior of the electron density distribution and extra ordinary waves both for collisional and collisionless cases at hmF2 peak in the ionosphere.

Key words: Ionosphere, Refractive Index, Equator Region

Ekvator Bölgesinde İyonosferin Kırılma İndisinin Mevsimsel Davranışı

Özet

Bu çalışmada, ekvator bölgesinde iyonosferin kırılma indisinin mevsimsel davranışı, dünyanın gerçek manyetik alan geometrisi kullanılarak hem çarpışmalı hemde çarpışmasız durumlarda, kuzey yarım küre için enleme göre çalışılmıştır. İyonosferin hmF2 (F2- bölgesinin tepe yüksekliği) de çarpışmalı ve çarpışmasız durum için elektron yoğunlu dağılımı ile extra-ordinary dalgının davranışı arasında bir uyum olduğu görülmüştür.

Anahtar Kelimeler: İyonosfer, Kırılma İndisi, Ekvator Bölgesi

1. Introduction

The ionosphere is the layer of the earth's atmosphere that extends from 50 to 1000 km. The ionosphere significantly affects the propagation of radio waves so the variability of the ionosphere is important for the ionospheric physics and radio communications. The ionosphere can be characterized with its electron density distribution which is a complex function of spatial and temporal variations, geomagnetic and solar activity. Usually, the ionosphere with respect to its electron density distribution is separated into five independent regions, sometimes called layers. The bottom one, from 50 to 80 km, is called D layer, from 80 to 130 km is the E layer, and above 150 km is F layer. The F region is usually separated at the F1 layer,

from 130 to 200-250 km, and the F2 layer is above 250 km [1]. The temporal and the spatial behaviors of the ionosphere depend on earth's diurnal and annual rotation and the distribution of the magnetic field lines of the magnetic dipole. Some of the studies in the literature [2-5] investigate the annual and the semiannual variations of the electron density profiles suggest that these ionospheric behaviors can cause deviations in the electron density distributions which are called as anomalies. The ionospheric anomalies generally arise because of the simple solar-controlled behavior. The principal anomalies observed at mid-latitudes may be characterized .Firstly, winter or seasonal anomaly: NmF2 is greater in winter than in summer by day, but the anomaly disappears at night, NmF2 being greater in summer than in

winter. The second, semiannual anomaly: NmF2 is greater at equinox than at solstice. Third, annual or non-seasonal anomaly; in the world as whole December NmF2 is on average greater than June NmF2, both by day and by night. The seasonal anomaly is greater in Northern than the Southern Hemisphere [3-7]. In addition to all above phenomena, the ionosphere may act as an efficient reflector with frequencies below 30 MHz, allowing high frequency (HF) radio communication to distances of many thousands of kilometers [8-15]. The radio waves show different behaviors depended on their frequencies, oscillation frequency of the electron and the refractive index of the ionospheric plasma [11-17]. Due to these behaviors, the wave reflects, refracts or absorbs from the ionosphere. Radio waves in the ionosphere are subject to some attenuation because the motions of the electrons and ions are damped through the collisions with other particles. In recent years, the information about the state of the Earth's ionosphere has been improved [12, 14, 15]. Hence, most of the used approximations for ionospheric calculations are unrealistic. To see the effects of the ionosphere on the wave propagation, more detailed theoretical investigation of the refractive index of ionosphere are needed [17]. There are some certain assumptions that the ambient magnetic field is unrealistic in the ionosphere in recent studies. However, as in the vertical and oblique sounding of the ionosphere by radio pulses, small differences can be important or sometimes necessary when high accuracy is required to allow for the refractive index or wave vector [15, 17] The most dramatic features of the solution are resonances and cut-offs. Resonances are characterized by a phase velocity going to zero ($v_p = \omega/k \rightarrow 0$) which is equivalent to the index refraction $n = kc/\omega$ going to infinity ($k \rightarrow \infty$). The wave energy is absorbed by ionospheric plasma at resonance points. Cut-offs are defined by index of refraction going to zero ($k \rightarrow 0$). At these cut-offs points, the wavelength goes to infinity and the waves are reflected. Cut-off points can be used for plasma density measurements [10, 11, 13, 14]. In this study, winter and seasonal anomaly effects on electron density distribution in the F2-layer and the refractive indices of HF waves traveling in a direction vertical to the

ionosphere are investigated as depending on various parameters in the ionosphere. The results are obtained for 38.7°N, 39.2°E geographical coordinates and for year 1996. The ionospheric parameters used in the study are obtained from IRI model. The method used in the study and the results are presented in Section 2 and 3, respectively.

2. Dispersion Relations

Assuming a plane wave solution, where the velocity and the fields vary as $\exp[i(\mathbf{k} \cdot \mathbf{r} - \omega t)]$, a general wave equation for electromagnetic waves can be defined as:

$$n^2 \mathbf{E} - \mathbf{n}(\mathbf{nE}) - \left[\mathbf{I} + \frac{i}{\epsilon_0 \omega} \sigma \right] \mathbf{E} = 0 \quad (1)$$

where \mathbf{n} ($=\mathbf{k}c/\omega$) is the refractive index, \mathbf{k} the wave vector, \mathbf{E} the electric field, \mathbf{I} the unit matrix, σ the conductivity tensor and ϵ_0 the free space electric permittivity coefficient. Equation (1) is the basic dispersion relation from where \mathbf{n} can be obtained in terms of plasma parameters. At high frequencies, the ratio between the electron collision frequency (ν) and the wave frequency (ω), that is Z ($=\nu/\omega$), is small and can often be neglected. However, small differences become relevant when higher accuracy is needed. In this study, a first approximation is made to include collisions in the calculation of \mathbf{n} . A vertical electromagnetic wave is considered, which travels in the z direction in the ionosphere. The z-axis is vertical with its origin located on the ground. The x and y axes indicate the geographic eastward and the northward in the northern hemisphere, respectively. Being I and d the magnetic dip and declination angles, respectively, the geomagnetic field in terms of its components is $\mathbf{B} = B_x \mathbf{a}_x + B_y \mathbf{a}_y + B_z \mathbf{a}_z$, where $B_x = B \cos(I) \sin(d)$, $B_y = B \cos(I) \cos(d)$, $B_z = B \sin(I)$. The travelling electromagnetic wave presents a component propagating in a direction perpendicular to the magnetic field and other along the magnetic field. In the first case, the ordinary (O) and extraordinary (X) waves with a refractive index (n_o and n_x) are defined by Equation (2) and Equation (3), respectively [15, 17]:

$$n_o^2 = 1 - \frac{X}{1+Z^2} + iZ \frac{X}{1+Z^2} \quad (2)$$

$$n_x^2 = 1 - \frac{X[(1-X)(1-X-Y^2\cos^2I\cos^2d)+Z^2]}{[1-X-Z^2-Y^2\cos^2I\cos^2d]^2+Z^2[2-X]^2} + iZ \frac{X[(1-X)^2+Z^2+Y^2\cos^2I\cos^2d]}{[1-X-Z^2-Y^2\cos^2I\cos^2d]^2+Z^2[2-X]^2} \quad (3)$$

In the case along the magnetic field, the circularly polarized waves with a refractive index (n_p) can be given as [10, 12]:

$$n_p^2 = 1 - \frac{X[1 \mp Y\sin I]}{[1 \mp Y\sin I]^2+Z^2} + iZ \frac{X}{[1 \mp Y\sin I]^2+Z^2} \quad (4)$$

Where the signs (-) and (+) correspond to right and left hand polarization, respectively. Equation (2), Equation (3) and Equation (4) are defined in terms of the magneto-ionic parameters X ($=\omega_p^2/\omega^2$), Y ($=\omega_c/\omega$) and Z ($=v/\omega$), where ω_p and ω_c are the plasma frequency and the electron gyro frequency, respectively. From these equations, the refractive index can be defined as $n^2 = (\mu + i\chi)^2 = M + iN$. The real part of n (μ) becomes as follows:

$$\mu^2 = \frac{1}{2} [(M^2 + N^2)^{1/2} + M] \quad (5)$$

For HF waves ($Z^2 \ll 1$), the expression $(1+Z^2)^{-1}$ in the refractive indices can be approximated to $(1-Z^2)$, by using binomial expansion and neglecting terms of order higher than Z^2 . By using these approximations, μ results for the ordinary, extraordinary and circularly polarized waves can be defined with $X' = X/[1-Y \sin I]$ and $Z' = Z/(1-Y \sin I)$ as follows [15]:

$$\mu_o^2 \approx (1-X) + Z^2 \frac{X(4-3X)}{4(1-X)} \quad (6)$$

$$\mu_x^2 \approx \frac{(1-X)^2 - Y^2\cos^2I\cos^2d}{1-X-Y^2\cos^2I\cos^2d} + Z^2 \frac{X^2[(1-X)^2 + Y^2\cos^2I\cos^2d]^2}{4[1-X-Y^2\cos^2I\cos^2d]^3 [(1-X)^2 - Y^2\cos^2I\cos^2d]} \quad (7)$$

$$\mu_p^2 \approx (1-X') + Z'^2 \frac{X'(4-3X')}{4(1-X')} \quad (8)$$

These equations hold for $X < 1$ and $X' < 1$. The collision frequency ν is the sum of ν_{ei} and ν_{en} , where ν_{ei} and ν_{en} are the electron-ion and the electron-neutral collision frequencies, respectively. These frequencies are given as follows [1]:

$$\nu_{ei} = N \left[59 + 4.18 \log \left(\frac{T_e^3}{N} \right) \right] \times 10^{-6} T_e^{-3/2} \text{ [m.k.s.]} \quad (9)$$

$$\nu_{en} = 5.4 \times 10^{-16} N_n T_e^{1/2} \text{ [m.k.s.]} \quad (10)$$

Where N is the electron density, N_n is the neutral particle density, and T_e is the electron temperature.

3. Numerical Analysis and Results

In this study, winter and seasonal anomaly effects on electron density distribution in the F2-layer and the refractive indices of HF waves traveling vertical into the ionosphere both for collisional and collisionless cases are investigated as depending on various parameters in the ionosphere. The results are obtained for geographic coordinates of 38.70 N, 39.20 E, $I=55.60$, $d=3^\circ$, $R=10$, $\omega=38.7 \text{ E}+6$ (rad/s) and for year 1996 by using Equations (2)-(8). The ionospheric parameters used for calculations are obtained by using IRI model. For given location, time and date, IRI model has described the electron density, electron temperature, ion temperature, and ion composition in the altitude range from about 50 km to about 2000 km; and also for the electron content. It provides monthly averages in the nonauroral ionosphere for magnetically quiet conditions. It is observed that

the maximum electron density is observed in equinoxes at midnight. In the solstices, maximum electron density is observed at noon. At midnight times, it is observed that electron density in December and March are greater than in June and September. It is also observed that refractive indices have similar values for the collisional and collisionless cases. When the electron density profiles and the refractive indices profiles are compared with each other's, it is observed that there is a harmony between the electron density and the real part of the refractive index of the x- wave in the height of the ionospheric F2-peak. But there is a dissonance between the other waves and both the electron density, hmF2 and the refractive index at the time (around 12 o'clock by day) when the winter anomaly take places. When the winter anomaly occurs (in December and March), all the refractive indices values of the extra ordinary

wave (n_x) obtained from Equation (3) both for collisional and collisionless cases have the minimum values in the ionospheric plasma. This result can be interpreted that the denominator of the collision term in Equation (7) decreases. Due to this; the real part (μ_x) of the refractive index of the x-wave seasonally increases at the height of the ionospheric F2-peak for winter anomaly case in the ionospheric plasma. In order to demonstrate this observation, electron density variations with latitudes in equinoxes 21 March and 23 September and solstices 21 December and 21 June for 12 o'clock and 24 o'clock are given in Figure 1 and Figure 2, respectively. It is observed from Figure 2b and Figure 2c that electron density values in 21 March at 24 o'clock and in June 21 at 12 o'clock are greater than from 21 December and 23 September in the ionospheric plasma. Minimum electron density is also observed from Figure 1a at 12 o'clock.

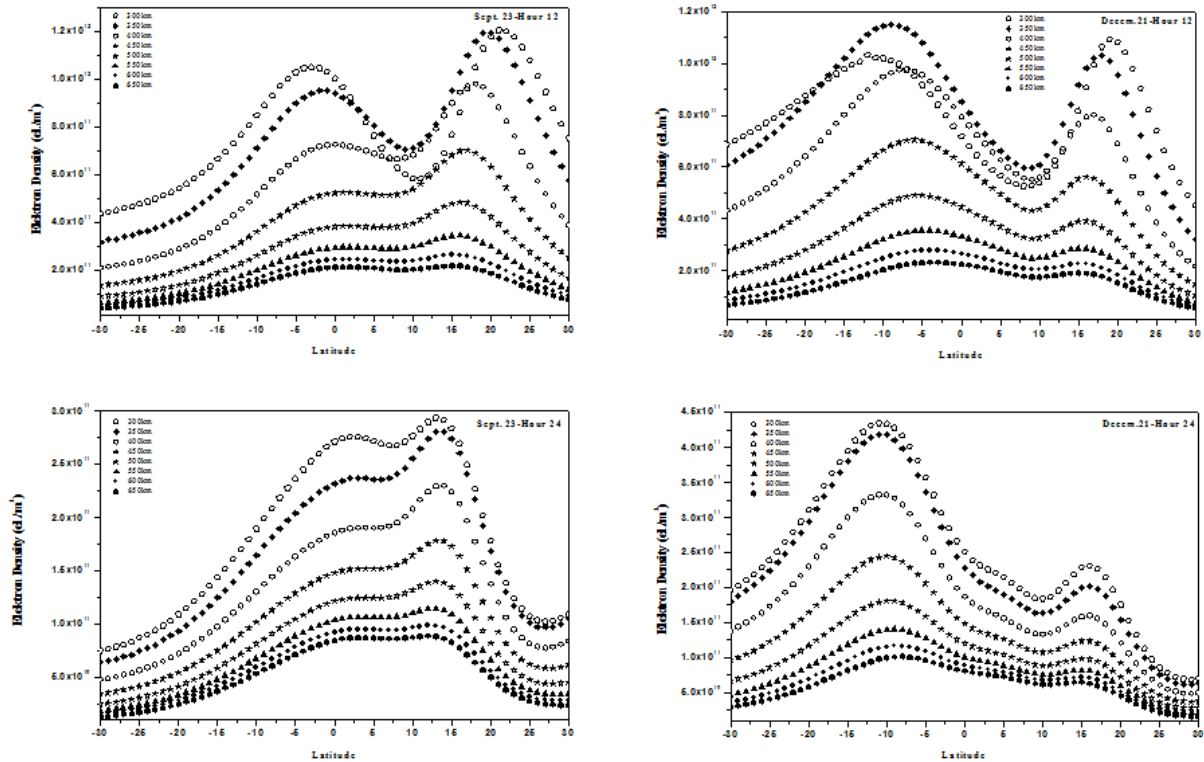


Figure 1. Electron density distributions at the heights from 300 km to 650 km for: a) September 23, 12 o'clock; b) December 21, 12 o'clock; c) September 23, 24 o'clock; d) December 21, 24 o'clock.

The Seasonal Behavior of the Refractive Index of the Ionosphere over the Equatorial Region

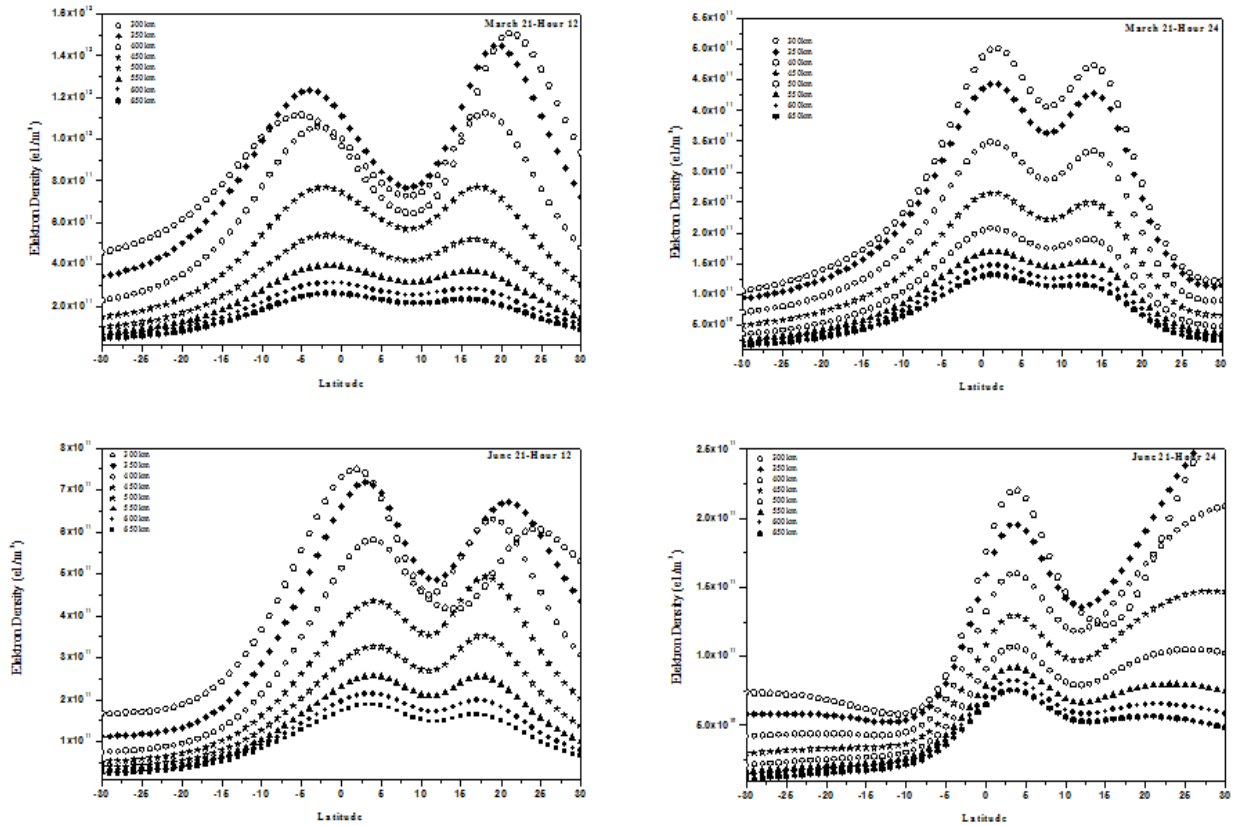


Figure 2. Electron density distributions at the heights from 300 km to 650 km for: a) March 21, 12 o'clock; b) March 21, 24 o'clock; c) June 21, 12 o'clock; d) June 21, 24 o'clock.

In order to demonstrate the harmony between the electron density and the refractive index, refractive indices values of the extra ordinary wave (n_x) are given in Figure 3 for September and December and in Figure 4 for March and June, respectively. When the Figure 1, Figure 2 and Figure 3 and Figure 4 are compared, symmetry is observed between the profiles of the electron density and refractive index. It is observed from Figure 3b, Figure 4a, Figure 5b

and Figure 6a, around 12 o'clock, when the winter anomaly occurs, refractive index values in both collisional and collisionless cases have been taking the minimum values both for collisional and collisionless cases. This result is depend on the behavior of the extra ordinary wave in collisional case with respect to other waves that displays a reverse behavior to the winter anomaly in the ionosphere plasma.

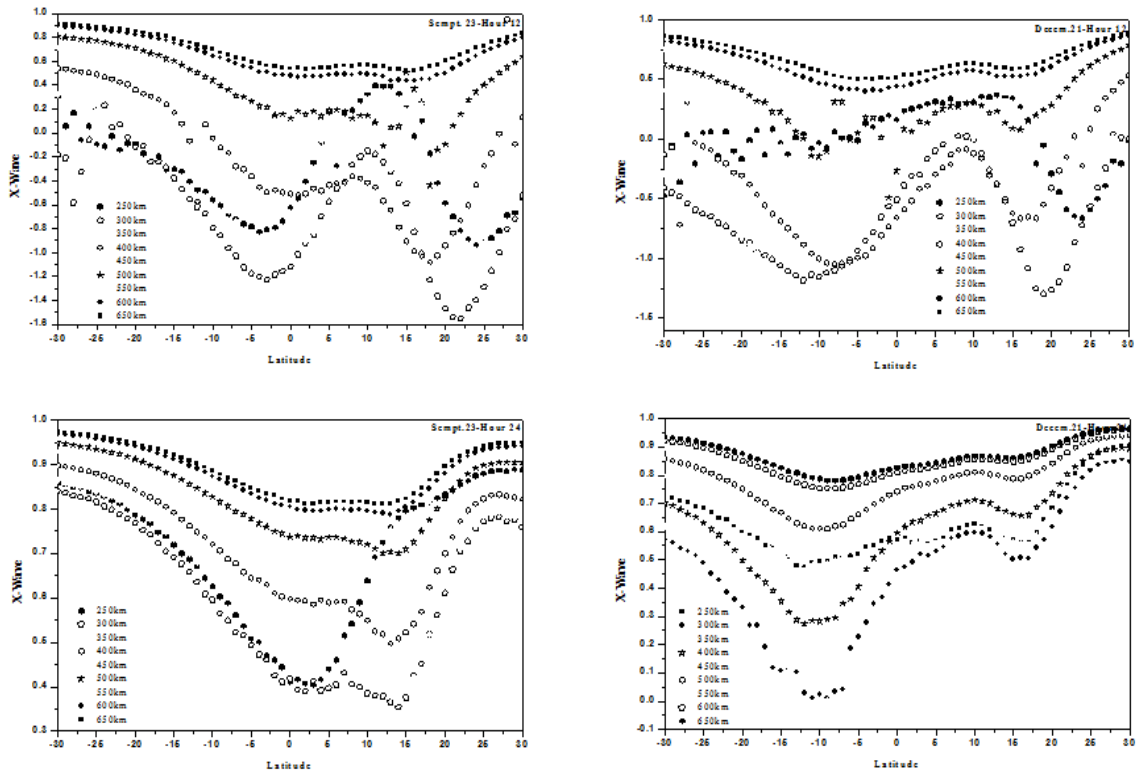


Figure 3. The refractive index values of the extra ordinary wave at the hmF2 peaks in the ionospheric plasma for the collisional case at the heights from 300 km to 650 km for: a) September 23, 12 o'clock; b) December 21, 12 o'clock; c) September 23, 24 o'clock; d) December 21, 24 o'clock.

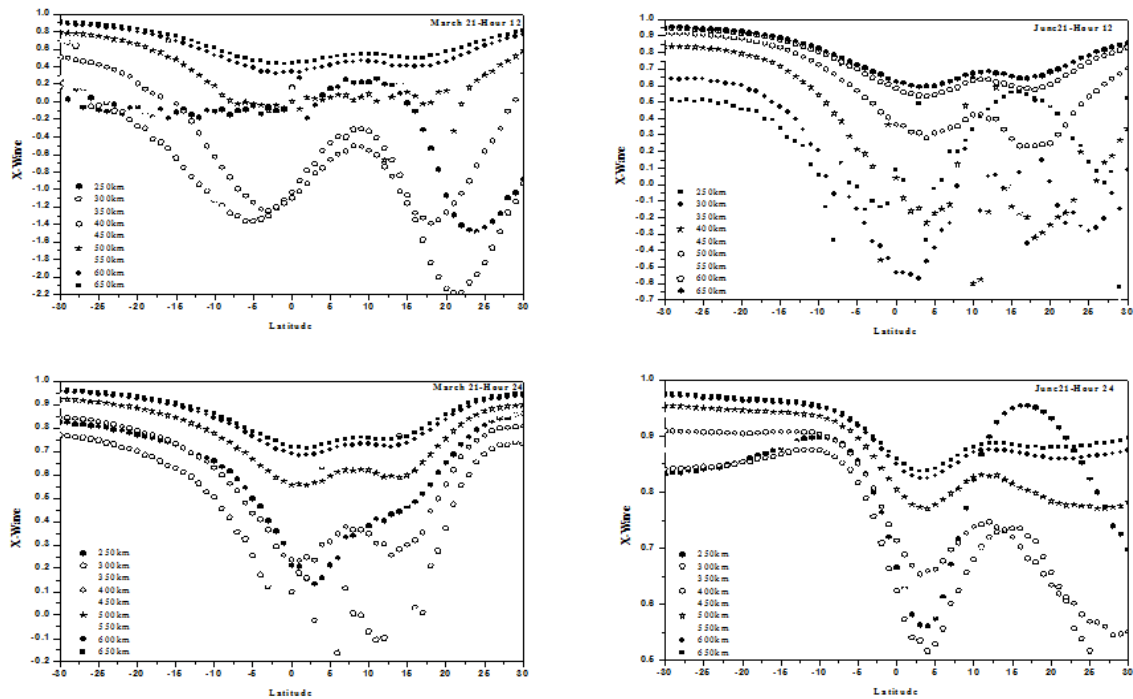


Figure 4. The refractive index values of the extra ordinary wave at the hmF2 peaks in the ionospheric plasma for the collisional case at the heights from 300 km to 650 km for: a) March 21, 12 o'clock; b) March 21, 24 o'clock; c) June 21, 12 o'clock; d) June 21, 24 o'clock.

The Seasonal Behavior of the Refractive Index of the Ionosphere over the Equatorial Region

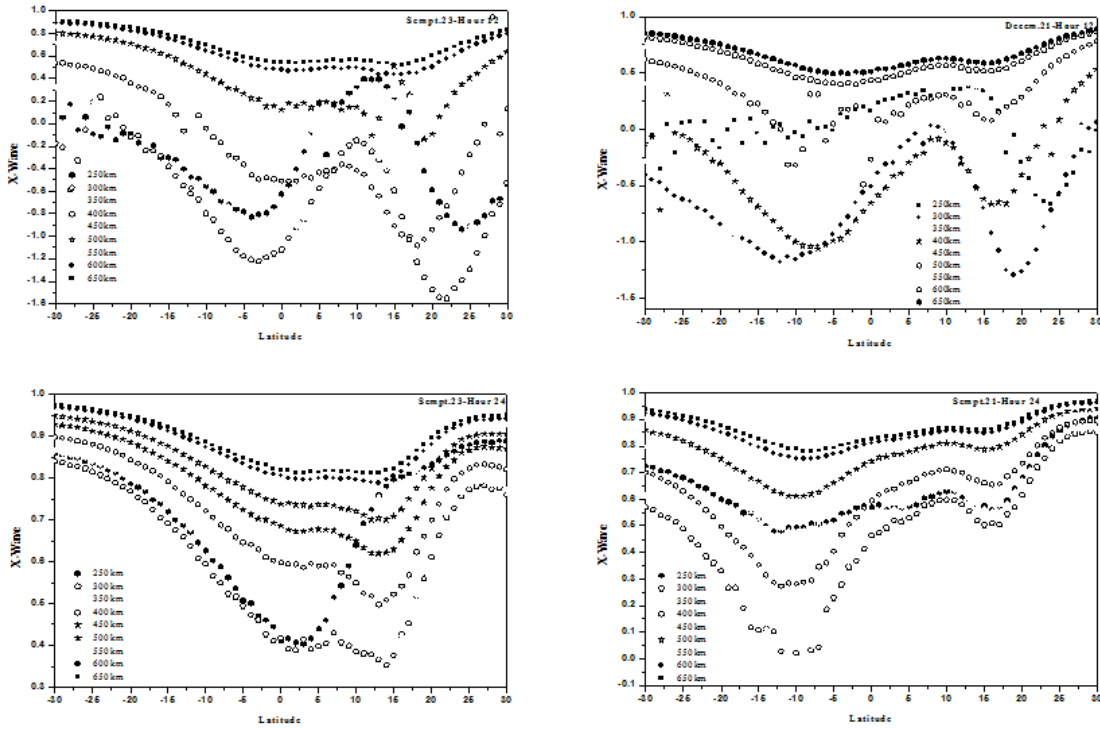


Figure 5. The refractive index values of the extra ordinary wave at the hmF2 peaks in the ionospheric plasma for the collisionless case at the heights from 300 km to 650 km for: a) September 23, 12 o'clock; b) December 21, 12 o'clock; c) September 23, 24 o'clock; d) December 21, 24 o'clock.

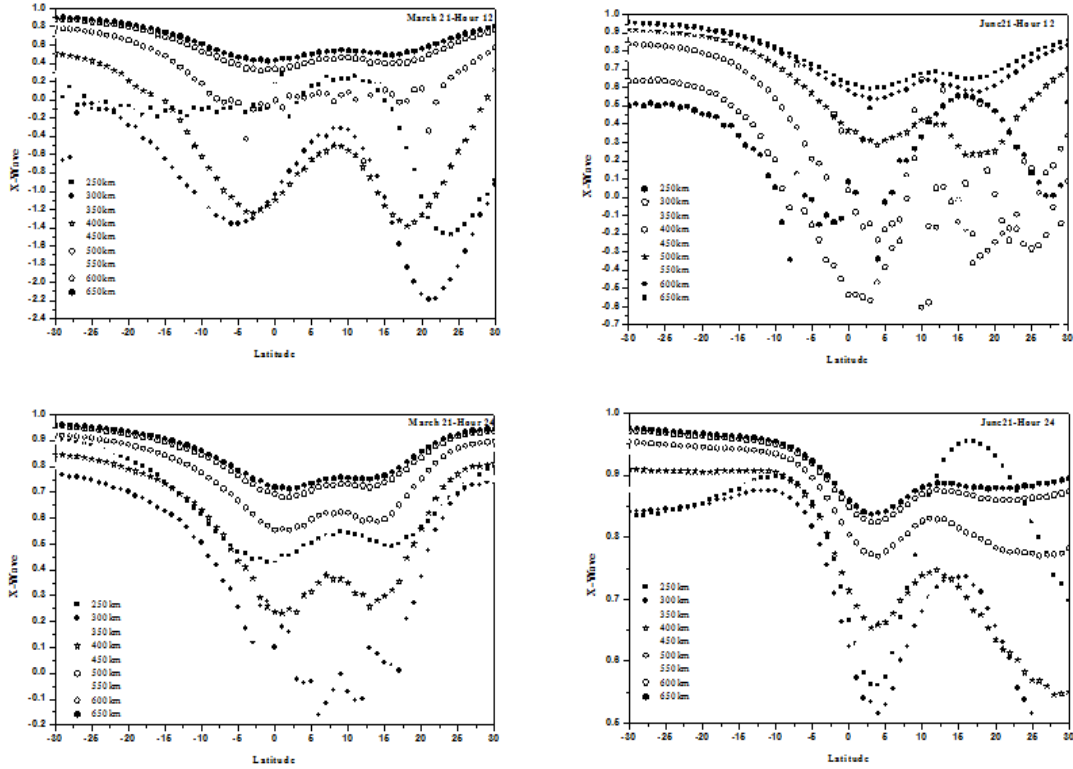


Figure 6. The refractive index values of the extra ordinary wave at the hmF2 peaks in the ionospheric plasma for the collisionless case at the heights from 300 km to 650 km for: a) March 21, 12 o'clock; b) March 21, 24 o'clock; c) June 21, 12 o'clock; d) June 21, 24 o'clock.

Finally, there is a dissonance between the electron density in height of the ionospheric F2-peak and the refractive indexes of the ordinary, the polarized and the extra ordinary waves for both collisional and collisionless cases except the real part (μ_x) of the refractive index of the x-wave at mid-latitudes in the ionospheric plasma. It is possible that this dissonance can result from the collision term in Equation (2) and Equation (4).

4. Conclusion

In this study, the effects of the winter or seasonal anomaly in height of the ionospheric F2-peak on the refractive index both for collisional and collisionless cases of HF waves traveling in a direction vertical to the ionosphere are investigated for mid-latitudes and midnight and noon hours in the equinoxes and solstices. It is observed that the winter anomaly only affects the real part (μ_x) of the refractive index of the extra ordinary wave for collisional and collisionless cases in height of the ionospheric F2-peak. There are dissonance between the electron density and the refractive index of the extra ordinary wave in height of the ionospheric F2-peak. But, there is seasonally an exact harmony between the electron density and the real part of the refractive index of the x-wave, except the other waves (ordinary and polarized waves). From these results, it is observed that in the case of high frequency waves traveling vertically into ionosphere, the phase velocity of all of the waves except the real part of the extra ordinary ($Z \neq 0$) increases at the time when the winter anomaly occurs. Due to this fact, the reflection heights of the all waves, except the real part of the extra ordinary ($Z \neq 0$), increases depending on the winter anomaly. The proposed procedure can be used in the assessments of the ionosphere variables, such as conductivity and it can be also used for ionospheric plasma density measurements. This study can become important in mid-latitude stations for ionosonda measurements because the refractive index of the medium determines the medium of behavior against any external influence.

5. References

1. Rishbeth, H. and O.K. Garriott, (1969), *Introduction to Ionospheric Physics*. Academic Press, New York and London, 331s.
2. Balan, N., Y. Otsuka, S. Fukao, M.A. Abdu and G.J. Bailey, (2000), Annual variations of the ionosphere: a review based on MU radar observations. *Advances in Space Research*, 25(1), 153-162.
3. Rishbeth, H., I.C.F. Müller-Wodarg, L. Zou, T.J. Fuller-Rowell, G.H. Millward, R.J. Moffett, D.W. Idenden and A.D. Aylward, (2000), Annual and semiannual variations in the ionospheric F2-layer. II. physical discussion. *Annales Geophysicae*, 18, 945-956.
4. Zou, L., H. Rishbeth, I.C.F. Müller-Wodarg, A.D. Aylward, G.H. Millward, T.J. Fuller-Rowell, D.W. Idenden and R.J. Moffett, (2000), Annual and semiannual variations in the ionospheric F2-layer I. modeling. *Annales Geophysicae*, 18, 927-944.
5. Bhuyan, P.K. and K. Bhuyan, (2008), The equatorial ionization anomaly at the topside F-region of the ionosphere along 75°E. *Advances in Space Research*, 43(2009), 1676-1682.
6. Rishbeth, H. (2006), F-region links with the lower atmosphere. *Journal of Atmospheric and Solar-Terrestrial Physics*, 71, 469-478.
7. Rishbeth, H. (2000), Semiannual and annual variations in the height of the ionospheric F2-peak. *Annales Geophysicae*, 18, 285-299.
8. Zhang, D.Y. (1991). New method of calculating the transmission and reflection coefficients and fields in a magnetized plasma layer. *Radio Science*, 26, 1415-1418.
9. Lundborg, B. and B. Thide, (1986), Standing wave pattern of HF radio waves in the ionospheric reflection regions 2 Applications. *Radio Science*, 21, 486-500.
10. Ratcliffe, J.A., (1959), *The Magneto-Ionic Theory and its Applications to the Ionosphere*. Cambridge University Press.
11. Budden, K.G., (1988), *The Propagation of Radio Waves*, Cambridge University Press.
12. Aydogdu, M. and O. Ozcan, (1996), Effects of magnetic declination on refractive index and wave polarization coefficients of electromagnetic waves in mid-latitude ionosphere. *Indian Journal of Radio and Space Physics*, 25, 263-270.
13. Hagfors, T., (1984), Electromagnetic wave propagation in a field-aligned-striated cold magnetoplasma with application to the ionosphere. *Journal of Atmospheric and Solar Terrestrial Physics*, 46, 211-216.
14. Al'pert, Ya. L., (1980), The direction of the group velocity of electromagnetic waves in a

- multicomponent magneto-active plasma in the frequency range $0 < \omega < \infty$. *Journal of Atmospheric and Solar Terrestrial Physics*, 42, 205-216.
15. Aydogdu, M., A. Yesil, and E. Guzel, (2003), The group refractive indices of HF waves in the ionosphere and departure from the magnitude without collisions. *Journal of Atmospheric and Solar Terrestrial Physics*, 66, 343-348.
 16. Atac, T., A. Ozguc, and R. Pektas, (2009), The variability of foF2 in different phases of solar cycle 23. *Journal of Atmospheric and Solar-Terrestrial Physics*, 71, 583-588.
 17. Aydogdu, M., E. Guzel, A. Yesil, O. Ozcan, and M. Canyilmaz, (2007), Comparison of the calculated absorption and the measured field strength HF waves reflected from the ionosphere. *Nouovo Cimento*, c, 243-253.